

Microencapsulation of Triglycidyl Isocyanurate by Solvent Evaporation Method for UV and Thermal Dual-Cured Coatings

Zhen Zhao, Xueqin Zhou, Qixiang Tian, Xiaoqing Wang, Wei Li, Dongzhi Liu

School of Chemical Engineering and Technology, Tianjin University, 300072 Tianjin, China

Correspondence to: D. Z. Liu (E-mail: dzliu@tju.edu.cn)

ABSTRACT: Triglycidyl isocyanurate (TGIC), a thermal curing agent, was encapsulated with poly(methyl methacrylate) with small particle size and narrow distribution for the application in acrylic resins to prepare one-package UV and thermal dual-cured coatings. Investigation of the wettability and thermal properties suggests that the microcapsules have better compatibility with acrylic resins and thermal stability as compared to pure TGIC. Results of the release performance experiments indicate good storage stability at 25°C and a quick release of vast TGIC at 120°C for the microcapsules. The UV-thermal dual-cured coatings prepared with the microcapsules exhibit a fast, even and complete hardening at 130°C together with an excellent adhesion to the mild steel panels. The results presented here show an application potential of the microcapsules in UV and thermal dual-cured paints. © 2014 Wiley Periodicals, Inc. *J. Appl. Polym. Sci.* **2014**, *131*, 41008.

KEYWORDS: coatings; kinetics; morphology; properties and characterization; resins

Received 28 February 2014; accepted 10 May 2014

DOI: 10.1002/app.41008

INTRODUCTION

UV curing technology has been applied widely in printing, adhesives, coatings, and electronic devices because of its fast reaction rate, low energy consumption, solvent-free curing, and low capital investment.^{1–3} However, UV reactions are restricted in the shadow area as well as the thick coatings. UV and thermal dual-cured coatings have been developed to conquer these problems by introduction of thermal curing agents and substitution of UV-cured resins for UV and thermal dual-cured resins, which are commonly functional acrylic resins. Complete hardening of the coatings is achieved quickly via first UV curing and then thermal curing.^{4–10} One issue caused by thermal curing agents is that the storage time is short due to slow polymerization reactions.^{11–14} Therefore for commercial products the thermal curing agent is packaged separately and the user should fully disperse it into the UV and thermal dual-cured resins before application. Microencapsulation of thermal curing agents can overcome this disadvantage and make one-package products possible.¹⁵

Microcapsules of isocyanates have been prepared with polyurethane, poly(urea–formaldehyde) (PUF) and bilayer polyurethane/poly(urea–formaldehyde) (PU/PUF) by *in situ* technique.^{16,17} These microcapsules have good adhesive ability with epoxy resins and are widely used with them. However, the dispersibility of the microcapsules in acrylic resins is very poor owing to their high hydrophilicity compared to the hydrophobic acrylates and their prepolymers. Poly(caprolactone) (PCL) and

poly(methyl methacrylate) (PMMA) as the shell materials can improve the compatibility of the microcapsules with hydrophobic resins.^{18–20} Another problem is that the hydrophilic thermal curing agents show a low compatibility with acrylic resins, resulting in an uneven hardening of the coatings as the microcapsules are destroyed. 2-Phenylimidazole (2-PhI), an oil soluble curing agent, is able to overcome the above problems, but it requires a long time to harden the coatings.²¹

Triglycidyl isocyanurate (TGIC, Figure 1) is a thermal curing agent with three epoxy groups and has been used in large scale in powder coatings and solder inks.^{22–24} Compared to common thermal curing agents such as amines and imidazoles, TGIC has better compatibility with acrylic resins and can harden the coatings within a relatively short period.^{25–28} For this research, TGIC was microencapsulated with PMMA and the feasibility of the PMMA/TGIC microcapsules in UV and thermal dual-cured coatings was evaluated. The particle size, core loading, shell thickness, and morphologies of the microcapsules were discussed. The compatibility and release performance were investigated in detail. Finally, the application potential of PMMA/TGIC microcapsules in UV and thermal dual-cured coatings was demonstrated.

EXPERIMENTAL

Materials

Poly(methyl methacrylate) (PMMA, $M_w = 5 \times 10^5 \sim 1.0 \times 10^6 \text{ g mol}^{-1}$) was purchased from Taiwan Chi Mei Industrial

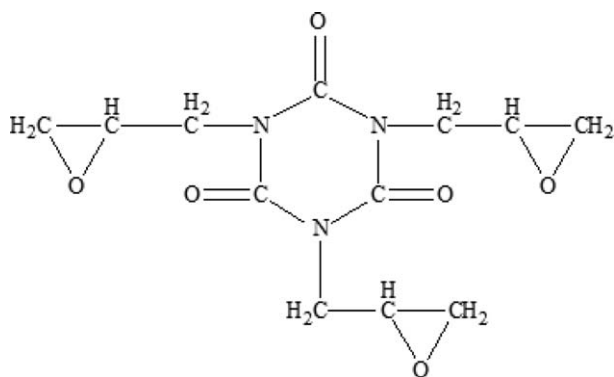


Figure 1. Structural formula of TGIC.

Corporation (China). TGIC (>99%) was supplied by Nanjing Fuxin Photoelectric Material Corporation (China). Dichloromethane (DCM), sodium dodecyl sulfate (SDS), acetonitrile (MeCN), and dimethylsulfoxide (DMSO) were obtained from Guang Fu Fine Chemical Research Institute (Tianjin, China). All the reagents were analytical-grade without further purification. Liquid photosensitive solder resist ink (LPSRI) was obtained from Rong Da Photographic Technology Corporation (Shenzhen, China) and contains 60% acrylic resins, 25% acrylate monomers, 5% photosensitizers, and 10% pigments.

Preparation of PMMA/TGIC Microcapsules

TGIC (2 g) was dispersed into the DCM solution (10 mL) of PMMA (0.5 g) on a ball mill (KEQ2L, Qidong Hong Hong instrument equipment factory) at 500 r/min for 50 min. 40 mL 1 wt % SDS aqueous solution was added slowly into the dispersion at a stirring rate of 300 rpm at 20°C. Then the stirring rate was improved to 2000 rpm and kept at 2000 rpm for 20 min at ambient temperature. Thereafter the agitation rate was decreased to 300 rpm and another 40 mL 1 wt % SDS aqueous solution was added into the emulsion. After a stirring at ambient temperature for 1 h, the resulted emulsion was heated to 35°C within 20 min and kept at 35°C for about 2 h under atmospheric pressure to remove most organic solvent. Then the system pressure was reduced to 0.01 KPa by a circulating water vacuum pump and kept at 35°C for another 4 h to remove the rest of the solvent. Finally, the PMMA/TGIC microcapsules, denoted as MC-1 were obtained by precipitation, decantation, and washing repeatedly with water, then dried at room temperature in a vacuum oven. PMMA/TGIC microcapsules MC-2 and MC-3 were obtained by the same procedure except that the PMMA amount was changed to 1 and 2 g, respectively.

Preparation of PMMA Microspheres

The preparation processes are the same as the microcapsules, except that the dispersion was replaced by the DCM solution (10 mL) of PMMA (0.5 g). The average size is 2.47 μm (Figure 2).

Preparation of UV and Thermal Dual-Cured Coatings

UV and thermal dual-cured paints were prepared by dispersing the PMMA/TGIC microcapsules or pure TGIC into LPSRI through via magnetic stirring at 100 rpm for 10 min. The microcapsules/LPSRI ratio was 20/100 by weight. Then, the

paints were coated onto mild steel panels by a glass bar at room temperature and exposed to the UV radiation for 5 min, followed by baking at 130°C for 10 min. The average UV light intensity at the samples was approximately 80 mW/cm² over the wave length range of 350–545 nm using a mercury UV lamp which was purchased from San Kun Technology Development Corporation. The microcapsules were replaced by pure TGIC to prepare comparable coatings and the TGIC/LPSRI ratio was 14.8/100 by weight to ensure the equal amounts of TGIC in the paints.

Characterization of Microcapsules and the Coatings

The surface morphology and size of the PMMA/TGIC microcapsules were analyzed with a scanning electron microscope (SEM, S4800, JP-Hitachi). The X-ray powder diffraction spectra (XRD, D-MAX2500, Rigaku) of TGIC and the microcapsules were collected by a D-MAX2500 diffractometer equipped with Cu K α ($\lambda = 1.5405\text{\AA}$) radiation in steps of 0.0833° with a step time of 1s over the 2θ range of 5° to 40° for each sample. The DSC curves were obtained on a thermal analyzer (DSC, Q20, TA Corporation) at a heating rate of 10°C/min. The thickness of coatings was measured by a Vernier caliper (1204-70, Ningbo Zhilin Testing Instrument Corporation). Mechanical properties of the coatings were measured by a pencil hardness instrument (QH-Q-A, Tianjin Fine Material Test Factory of China) and a coating adhesion instrument (QFZ, Tianjin Fine Material Test Factory of China) according to testing standards GB6739–86 and GB/T1720–88, respectively.

Determination of the Core Loadings

A 0.5 g dried microcapsules was cracked by squeezing, and then the TGIC was extracted with MeCN–waters (60 : 40) (10 mL \times 5). Residual shells were collected, dried, and weighed. The core (TGIC) loading in the microcapsules ($C_c\%$) is calculated as follows:

$$C_c\% = (1 - W_p/W_t) \times 100\% \quad (1)$$

where W_p and W_t are the weights of the residual shell and the dried microcapsules, respectively.

Wettability Determination

PMMA solutions were obtained by dissolving certain amount (0.5, 1, and 2 g) of PMMA in 10 mL DCM. Then the same amounts of these solutions were taken on the slides. As the solvent evaporates naturally, PMMA films with different thicknesses were formed, denoted as PMMA-1, PMMA-2, and PMMA-3. The thickness was estimated via volume and spreading areas. The contact angle was measured by dropping MMA on the films using Contact Angle Analyzer (Zhong Chen Digital Technology Apparatus Corporation). The TGIC film was prepared via pelleting method on a powder pressing machine (ZP9ZP7, Tiankang Pharmaceutical Machinery) and the compressive process was conducted under an applied pressure of 20 KPa for 5 min.

Release Experiments of the Microcapsules

The release experiments were carried out at 25 and 120°C, respectively. A 250 mL round bottomed flask was filled with 200 mL of MeCN–waters (60 : 40, in volume) solution and 0.10 g of the TGIC/PMMA microcapsules was added into the

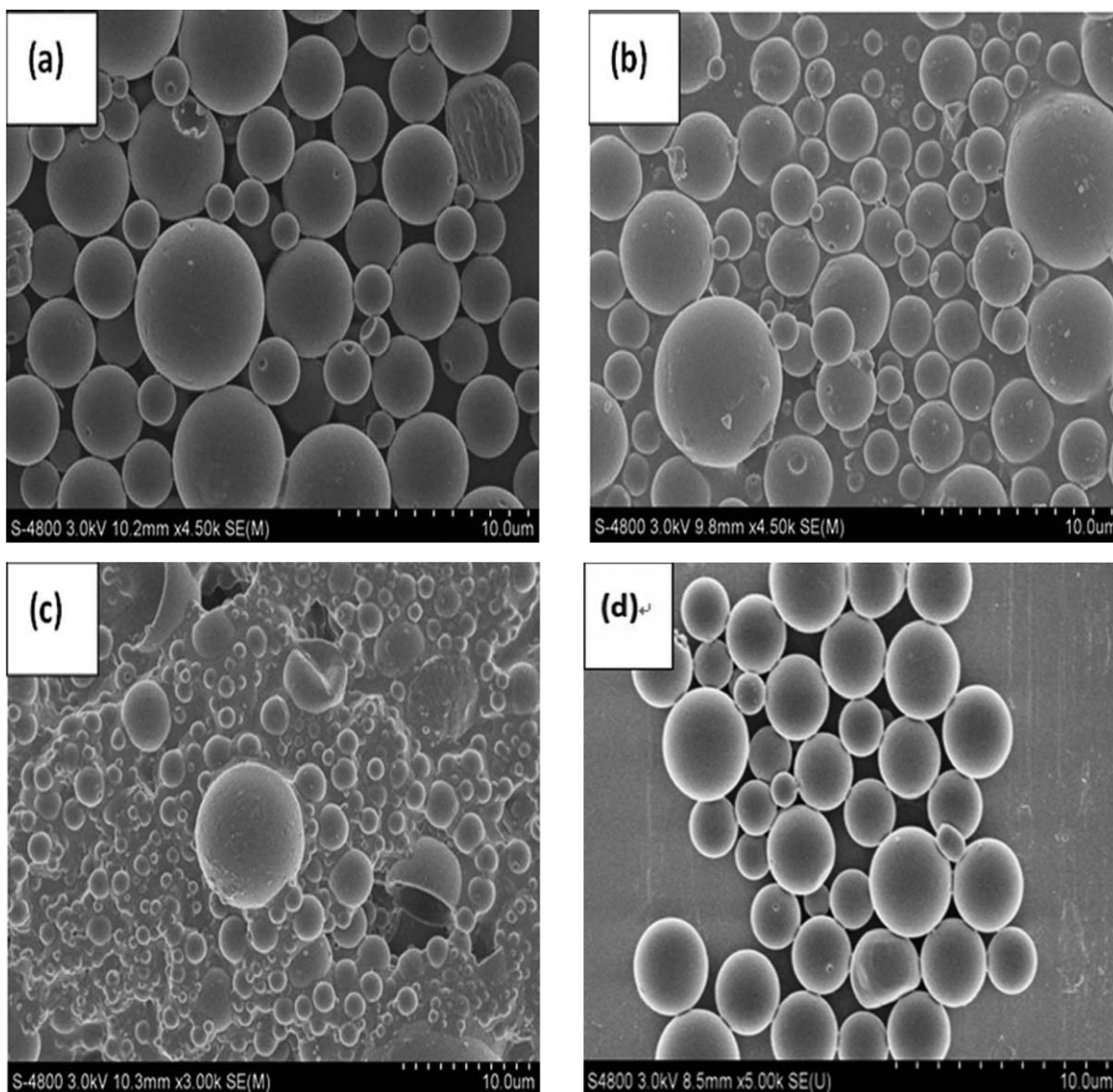


Figure 2. SEM images of PMMA/TGIC microcapsules (a) MC-1, (b) MC-2, (c) MC-3, and (d) PMMA microspheres.

solution at 25°C. The dispersion was stirred at 25°C with a magnetic stir bar at a very slow speed (60 rpm). Then, 1 mL of the sample solution was collected from the upper part of the solution at determined intervals for measurement and the same volume MeCN–waters (60 : 40) solution was replenished to ensure the same amount of the solution. For the high temperature experiments, 0.10 g of TGIC/PMMA microcapsules was added into 10 mL DMSO at 120°C and kept for 5 min, then 200 mL MeCN–waters (60 : 40) solution was added to dilute the solution. Afterwards, 1 mL of the sample solution was collected from the upper part of the solution for measurement.

Absorbance of the samples at 210 nm was measured on a UV-Vis spectrometer (EVOLUTION300, Thermo Electron Corporation). The standard curve of TGIC solution in the mixture of MeCN–waters (60 : 40) was determined and the standard curve was acquired as the following: $A = 3.9386 \times 10^{-4} C + 2.9582 \times 10^{-6}$ ($r = 0.99966$, $P < 0.0001$, concentration range: $1 \times$

$10^{-4} \sim 5 \times 10^{-2}$ g/mL) where A and C are the absorbance and the concentration of TGIC solutions, respectively. The TGIC cumulative release amount of PMMA/microcapsules (R_a) is calculated as follows:

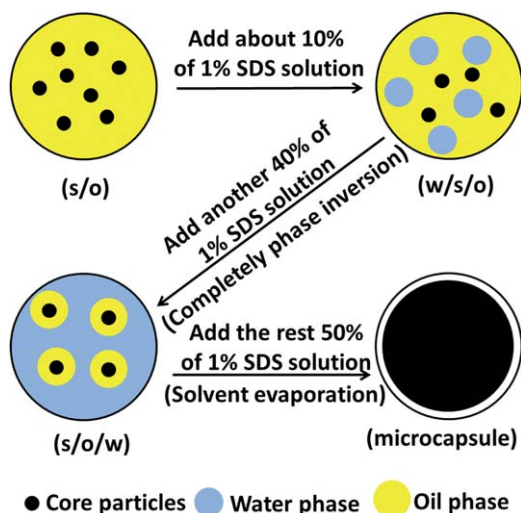
$$R_a = A_t / A_m \quad (2)$$

where A_t and A_m are the absorbance of sample solutions at determined intervals and absorbance obtained from the standard curve corresponding to a TGIC concentration of calculation from TGIC loading in the microcapsules, respectively.

RESULTS AND DISCUSSION

Formation of PMMA/TGIC Microcapsules

PMMA/TGIC microcapsules can be prepared either from MMA by *in situ* polymerization or from PMMA by solvent evaporation method. The microcapsules produced by the former process show larger size and wider distribution than that prepared



Scheme 1. Schematic illustration for the microcapsules formation process. [Color figure can be viewed in the online issue, which is available at wileyonlinelibrary.com.]

in the latter way. Large microcapsules are hard to be dispersed evenly in the resins, leading to an incompletely or partly solidifying phenomenon.²⁹ Moreover, the shell thickness of microcapsules can be easily controlled by solvent evaporation method.³⁰ As TGIC was insoluble in common solvents, including DCM, trichloromethane, methanol, dioxane, and 1,2-dichloroethane. In order to avoid using large quantities of solvents and improve the process efficiency, S/O/W emulsion method was used instead of simple organic solution to prepare PMMA/TGIC microcapsules.

As shown in Scheme 1, TGIC was first dispersed into the PMMA–DCM solution to form S/O dispersion. A ball-milling process was employed to get fine particles. Afterwards about 10% of 1 wt % SDS aqueous solution was introduced in this dispersion to form W/S/O emulsion. Then about 40% of 1 wt % SDS aqueous solution was added slowly into this W/S/O emulsion to achieve a phase reversion. Thereafter another 50% of 1 wt % SDS aqueous solution was employed to dilute the emulsion for solvent evaporation. SDS was used as an emulsion stabilizer in all of the process. Oil/water interfacial tension achieved low minimum during the process, so the size of the dispersed phase is small and narrowly distributed.³¹ Eventually, microcapsules with small particle size and narrow distribution were obtained.

Table I. Properties of PMMA/TGIC Microcapsules of Different Mass Ratio

| Sample | Initial addition | | Mass ratio of PMMA/TGIC | TGIC content ^a (%) | C_c^b (%) | E_c^c (%) | t_c^d (μm) | R_{σ}^e (%) (25°C) | R_{σ}^e (%) (120°C) |
|--------|------------------|----------|-------------------------|-------------------------------|-------------|-------------|---------------------------|---------------------------|----------------------------|
| | PMMA (g) | TGIC (g) | | | | | | | |
| MC-1 | 0.50 | 2.0 | 1/4 | 80.0 | 74.24 | 92.85 | 0.48 | 14.5 | 90.01 |
| MC-2 | 1.0 | 2.0 | 2/4 | 66.7 | 63.96 | 95.89 | 0.84 | 11.4 | 81.3 |
| MC-3 | 2.0 | 2.0 | 4/4 | 50.0 | 24.23 | 48.46 | 1.30 | 20.5 | 84.1 |

^a Initial TGIC content, which is the ratio of the weight of the initial addition of TGIC to the total addition of TGIC and PMMA.

^b Core (TGIC) loading in microcapsules calculated from eq. (1).

^c Encapsulation efficiency calculated from eq: C_c^b (%) / TGIC content^a (%).

^d Shell thickness calculated from eq. (3).

^e The TGIC cumulative release amount calculated from eq. (2).

Characterization of the PMMA/TGIC Microcapsules

The average size, core loading and shell thickness are shown in Table I. The average size of obtained microcapsules is between 2 and 4 μm . SEM images (Figure 2) show that all microcapsules are less than 5 μm . These results confirm small particle size and narrow distribution for PMMA/TGIC microcapsules. The core loading is lower than the initial TGIC content. This is attributed to the enhanced solubility of TGIC in water by the surfactant SDS. For a mononuclear PMMA/TGIC microcapsule with a core loading of $C_c\%$, the shell thickness (t) can be calculated using eq. (3), where R is the microcapsule radius and ρ_c and ρ_m are the densities of the TGIC cores and PMMA shells respectively. Hence microcapsules with different shell thickness can be produced by controlling the PMMA/TGIC ratio.

$$t = \left[1 - \left(\frac{C_c\% / \rho_c}{(1 - C_c\%) / \rho_m + C_c\% / \rho_c} \right) \right] R \quad (3)$$

The mass ratio of PMMA to TGIC also affects the morphology of the microcapsules. As shown in Figure 2, MC-1 and MC-2 are completely regular spherical microcapsules with smooth surface; while clear adhesion among microcapsules and poor encapsulation were observed for MC-3. It is probably because that the increased viscosity of the oil phase at high PMMA/TGIC ratio leads to vast polymers phase migration and impedes the solvent removal, which is not conducive to the formation of microcapsules.

Compatibility of PMMA/TGIC Microcapsules with Acrylic Resins

The shell material determines the compatibility between microcapsules and the acrylic resin. The wettability of MMA on PMMA films can reveal the compatibility of PMMA/TGIC microcapsules with acrylic resins.³² As shown in Table II, the contact angles between MMA and PMMA films are clearly less than the value between MMA and TGIC (20.01°), indicative of better wettability of MMA on PMMA than on TGIC. This can be reasonably explained by the higher structural similarity of PMMA to MMA compared to TGIC. Moreover, the contact angles decrease with the increased thickness of PMMA films. The results indicate that the thicker the shell thickness the better the compatibility and possibly the better dispersibility of microcapsules in acrylic resins.

Thermal Analysis and Crystal Structure of the Microcapsules

The DSC curves of TGIC and the microcapsules are shown in Figure 3. TGIC shows an endothermic peak at 101.49°C

Table II. Contact Angles Between MMA and TGIC film, PMMA Films of Different Thickness

| Sample | Film thickness (mm) | Contact angle (θ) ^a |
|-------------------|---------------------|---|
| TGIC ^b | 0.51 | 20.01 ± 0.38 |
| PMMA-1 | 0.27 | 18.78 ± 0.25 |
| PMMA-2 | 0.54 | 14.97 ± 0.31 |
| PMMA-3 | 1.08 | 9.33 ± 0.40 |

^aThe data are an average of five determinations results.

^bTGIC film was tableted by a powder pressing machine.

corresponding to the melting temperature of TGIC (101.5°C). This temperature is increased by 7–15°C for the microcapsules as the PMMA/TGIC ratio is enhanced from MC-1 to MC-3. The endothermic peak of MC-3 is at 114.9°C, close to T_g of PMMA microspheres (115.0°C). The enthalpy of the microcapsules is also less than that of pure TGIC and reduces obviously with the increased PMMA/TGIC ratio, which is attributed to the decreased TGIC loading. Another possible reason is that the crystal transformation of TGIC in the process of microcapsule preparation, which has been confirmed by XRD results.

Figure 4 provides the XRD spectra of PMMA/TGIC microcapsules MC-1, pure TGIC, PMMA microspheres and 1 : 4 mixtures of PMMA microspheres.

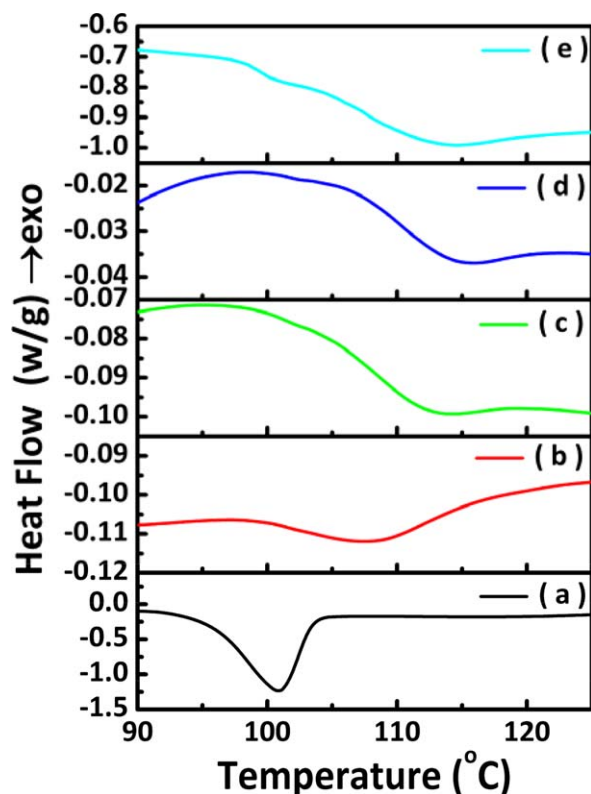


Figure 3. DSC curves of (a) pure TGIC, (b) MC-1, (c) MC-2, (d) MC-3, and (e) PMMA microspheres. [Color figure can be viewed in the online issue, which is available at wileyonlinelibrary.com.]

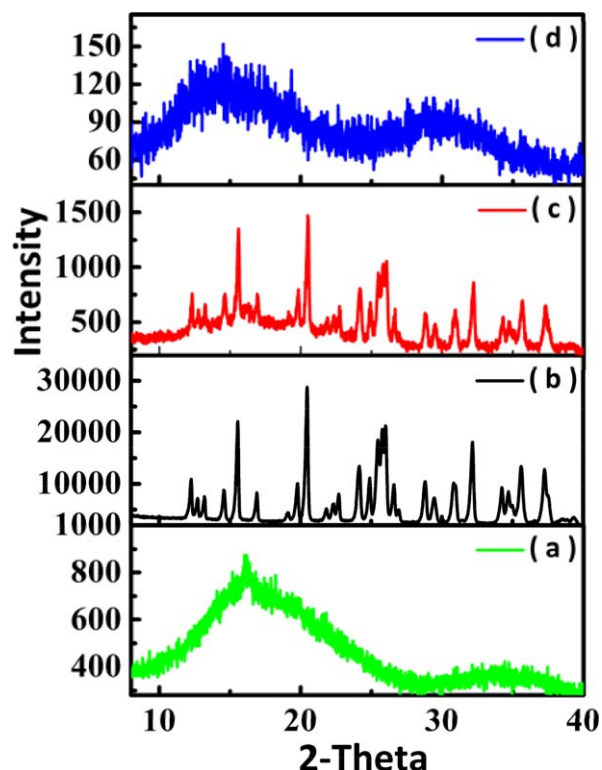


Figure 4. X-ray diffraction pattern of (a) MC-1, (b) TGIC, (c) 1:4 mixtures of PMMA microspheres and TGIC, and (d) PMMA microspheres. [Color figure can be viewed in the online issue, which is available at wileyonlinelibrary.com.]

ters of the hexagonal and orthorhombic crystallinity.³³ The presence of PMMA could not affect the crystallinity of TGIC for similar peaks in the XRD spectrum of the mixture as pure TGIC. However, the PMMA/TGIC microcapsules do not show any sharp crystallization peaks, indicating an amorphous state for TGIC inside the microcapsules. Similar crystal transformation was also found during ball milling process of azo pigment and trehalose.^{34,35}

Release Performance of the PMMA/TGIC Microcapsules

The release performance of the microcapsules was determined at both 25 and 120°C to analyze the storage stability and application feasibility of the microcapsules. As shown in Figure 5, at room temperature, initial TGIC release rates from the microcapsules were very high due to some free TGIC on the microcapsule surfaces. The release rates began to decrease 1 day later. After 10 days, no more TGIC was detected to be released from the microcapsules, indicative of a good sealing performance of PMMA/TGIC microcapsules for a long-term storage. Relative cumulative release amounts (R_a) of the microcapsules kept at 25°C for 40 days are listed in Table I. The highest R_a values were found as 20.5% for MC-3, corresponding to its poor encapsulation efficiency. R_a values of MC-1 and MC-2 are 14.5 and 11.4% respectively. R_a values of the microcapsules at 120°C for 5 min are also given in Table I and above 80% for all microcapsules, indicating a quick release of TGIC at 120°C. The R_a values have further reached 100% within 10 min for all microcapsules.

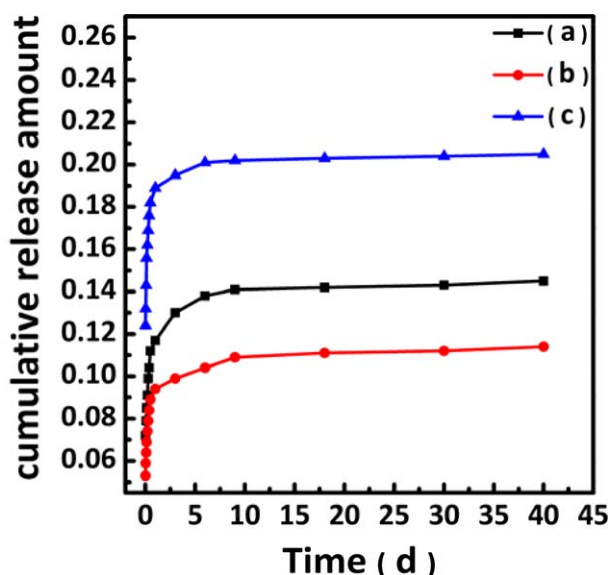


Figure 5. Plots of cumulative release amounts from PMMA/TGIC microcapsules: (a) MC-1, (b) MC-2, and (c) MC-3 at 25°C again the time. [Color figure can be viewed in the online issue, which is available at wileyonlinelibrary.com.]

Commonly a thicker shell corresponds to better barrier property as well as slower release property. However, MC-3 shows higher R_a values than MC-2 though the shell is thicker for MC-3

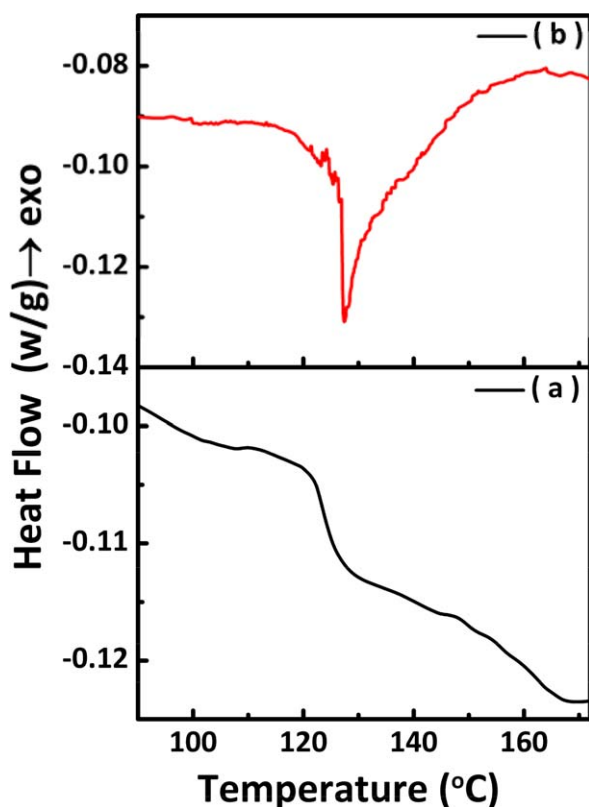


Figure 6. DSC curves for UV and thermal dual-cured coatings prepared with (a) MC-1 and (b) pure TGIC. [Color figure can be viewed in the online issue, which is available at wileyonlinelibrary.com.]

Table III. Hardness and Adhesion of UV and Thermal Dual-Cured Coatings^a

| Sample | Mass ratio of curing agent/acrylic resins | Pencil hardness | Adhesion to mild steel panels |
|------------|---|-----------------|-------------------------------|
| TGIC/LPSRI | 20/100 | 6H | 1 |
| MC-1/LPSRI | 14.8/100 | 6H | 2 |

^aThe thickness of coatings is 0.80 ± 0.05 mm.

(Table I). This is attributed to the free TGIC remained in microcapsule products. At room temperature, the initial R_a are primary due to the dissolution of the free TGIC. Results in Figure 5 and Table I indicate that the free TGIC amount is higher as the encapsulation efficiency is lower. The free TGIC adsorbed on microcapsule surfaces will dissolve in the solvent during the release experiments, resulting in a higher R_a values of MC-3 than of MC-2. However, for the experiments at 120°C, most TGIC was released from the microcapsules, leading to the highest R_a values for MC-1.

Curing Process and Mechanical Property of the Coatings

Previous results reveal that the PMMA/TGIC microcapsules might be a potential additive to produce one-package UV and thermal dual-cured coatings. Thus microcapsules MC-1 were added into a commercial acrylic resin LPSRI. The thermal curing process of the coatings was investigated by DSC measurements (Figure 6). The system prepared with pure TGIC was also studied in comparison. The curing reaction in both systems began to occur at around 100°C and corresponding exothermic peak overlaps with the endothermic peak of TGIC, leading to a higher endothermic peak (around 128°C) of the coatings than that of the additives (free microcapsules or TGIC). In addition, the appearance of endothermic peaks is an indication of complete melting of TGIC. Therefore, the post thermal heat-treatment temperature was set at 130°C. Combining with the above results, we assume the appearance of endothermic peaks as an indicative of complete melting and quick release of TGIC from the microcapsules. Therefore, the post thermal heat-treatment temperature was set at 130°C. Then the curing process of UV and thermal dual-cured coatings was specified as 5 min exposure to UV lights followed by 10 min baking at 130°C. As-prepared coatings are uniform with a thickness of 0.80 ± 0.05 mm and the mechanical properties are provided in Table III. The coatings prepared with MC-1 exhibit a same pencil hardness of 6H at all measured points as those prepared with pure TGIC, confirming the DSC results. In comparison, the coatings cured only at 130°C require a curing time of more than 30 min to achieve high pencil hardness. Besides, the coatings prepared with MC-1 show better adhesion to the mild steel panels than those prepared with pure TGIC.

CONCLUSIONS

The PMMA/TGIC microcapsules have been prepared by a solvent evaporation method using S/O/W emulsion. The ball-milling and phase inversion techniques were employed to

achieve microcapsules with small particle size and narrow distribution. Compared to pure TGIC, the PMMA/TGIC microcapsules have better compatibility with acrylic resins, higher thermal stability and less heat of fusion. The PMMA/TGIC mass ratio plays a key role on the morphologies and shell thickness of microcapsules, and therefore affects the compatibility, thermal stability and release performance. The thicker the shell the higher the compatibility and the less the heat of fusion. The microcapsules show good storage stability at 25°C and a quick release of vast TGIC at 120°C, leading to a fast, even, and complete hardening of the as-prepared UV-thermal dual-cured coatings. The coatings also exhibit excellent adhesion to the mild steel panels. The results presented here show the application potential of the PMMA/TGIC microcapsules in UV and thermal dual-cured paints.

REFERENCES

1. Park, C. H.; Lee, S. W.; Park, J. W.; Kim, H. *J. React. Funct. Polym.* **2013**, *73*, 641.
2. Lee, S. W.; Park, J. W.; Park, C. H.; Lim, D. H.; Kim, H. J.; Song, J. Y.; Lee, J. H. *Int. J. Adhes. Adhes.* **2013**, *44*, 138.
3. Park, Y. J.; Lim, D. H.; Kim, H. J.; Park, D.; Sung, I. K. *Int. J. Adhes. Adhes.* **2009**, *29*, 710.
4. Park, S. C.; Kim, H. K.; Hong, J. W. *Macromol. Res.* **2008**, *16*, 128.
5. Treya, S. M.; Sidenvalla, P.; Alavib, K.; Daniel Ståhlberg, D.; Mats Johansson, M. *Prog. Org. Coat.* **2009**, *64*, 489.
6. Narayanan, J.; Jungman, M. J.; Patton, D. L. *React. Funct. Polym.* **2012**, *72*, 799.
7. Sangermano, M.; Colucci, G.; Fragale, M.; Rizza, G. *React. Funct. Polym.* **2009**, *69*, 719.
8. Zhi, J.; Yong, H.; Ming, X.; Jun, N. *Prog. Org. Coat.* **2009**, *66*, 35.
9. Lee, S. W.; Park, J. W.; Kim, H. J.; Kim, K. M.; Kim, H. I.; Ryu, J. M. *J. Adhes. Sci. Technol.* **2012**, *26*, 317.
10. Hwang, H. D.; Kim, H. *J. React. Funct. Polym.* **2011**, *71*, 655.
11. Belbekhouche, S.; Ali, G.; Dulong, V.; Picton, L.; Cerf, D. L. *Carbohydr. Polym.* **2011**, *86*, 304.
12. Fuensant, M.; Grau, A.; Romero-Sánchez, M. D.; Guillem, C.; López-Buendía, A. M. *Polym. Bull.* **2013**, *70*, 3055.
13. Feng, J. Y.; Gao, L. J.; Chen, B.; Wu, X. J.; Luo, Q. L.; Wu, C. Y.; Zheng, C. X.; Lin, L. Z.; Deng, S. L.; Huang, X. M. *Carbohydr. Lett.* **2013**, *42*, 714.
14. Lacoangeli, T.; Chiavarini, M.; Fazio, A.; Marchetti, M.; Ciottoli, G. B. U.S. Patent 13, 990,974, Oct 3, **2013**.
15. Yin, T.; Rong, M. Z.; Zhang, M. Q.; Yang, G. C. *Compos. Sci. Technol.* **2007**, *67*, 201.
16. Credico, B. D.; Levi, M.; Turri, S. *Eur. Polym. J.* **2013**, *49*, 2467.
17. Huang, M.; Yang, J. *J. Mater. Chem.* **2011**, *21*, 11123.
18. Ham, Y. R.; Lee, D. H.; Kim, S. H.; Shin, Y. J.; Yang, M.; Shin, J. S. *J. Ind. Eng. Chem.* **2010**, *16*, 728.
19. Shin, M. J.; Shin, Y. J.; Hwang, S. W.; Shin, J. S. *J. Appl. Polym. Sci.* **2013**, *129*, 1036.
20. Li, Q.; Mishra, A. K.; Kim, N. H.; Kuila, T.; Lau, K.; Lee, J. H. *Compos. Part B.* **2013**, *49*, 6.
21. Xu, H.; Fang, Z.; Tong, L. *J. Appl. Polym. Sci.* **2008**, *107*, 1661.
22. Liu, S.; Tan, Y.; Shao, S.; Hui, Y.; Peng, H. *Adv. Mater. Res.* **2013**, *746*, 23.
23. Han, J.; Liang, G.; Gu, A.; Ye, J.; Zhang, Z.; Li, Y. *J. Mater. Chem. A* **2013**, *1*, 2169.
24. Xiong, J.; Jin, Y.; Shentu, B.; Weng, P. *J. Coat. Technol. Res.* **2013**, *10*, 621.
25. Kun, W.; Kandola, B. K.; Kandare, E.; Yuan, H. *Polym. Compos.* **2011**, *32*, 378.
26. Tai, X.; Chen, G. J.; Cao, Y.; Fan, L. Q. U.S. Patent 13,696,499, Jul 3, **2013**.
27. Fuke, K.; Taniguchi, T.; Ota, T.; Ito, H. U.S. Patent 13,403,422, Aug 30, **2012**.
28. You, J.; Lou, L.; Yu, W.; Zhou, C. *J. Appl. Polym. Sci.* **2013**, *129*, 1959.
29. Rule, J. D.; Sottos, N. R.; White, S. R. *Polymer* **2007**, *48*, 3520.
30. Wang, X.; Liu, D.; Li, W.; Tian, Q.; Zhou, X. *Mol. Cryst. Liq. Cryst.* **2013**, *571*, 57.
31. Saito, H.; Shinoda, K. *J. Colloid Interface Sci.* **1970**, *32*, 647.
32. Zhang, Q.; Liu, L. *Chem. J. Chin. Univ.* **2006**, *27*, 790.
33. Beyer, H.; Sajó, I.; Szegedi, A.; Vargha, V. *Eur. Polym. J.* **2007**, *43*, 4762.
34. Aruga, T.; Ohta, K.; Sasaki, M. U.S. Patent 5,863,683, Jan 26, **1999**.
35. Willart, J.; Gussemé, A.; Hemon, S.; Odou, G.; Danede, F.; Descamps, M. *Solid State Commun.* **2011**, *119*, 501.